

## SIMULATIONS OF THE ONSET OF TRANSIENT CONVECTION IN POROUS MEDIA UNDER FIXED SURFACE TEMPERATURE BOUNDARY CONDITION.

Ka Kheng, TAN and Torng, SAM

Department of Chemical and Environmental Engineering,  
 Universiti Putra Malaysia, 43400 UPM, Serdang, Selangor, Malaysia

### ABSTRACT

The theory of transient convection in porous media is advanced and verified by simulations using a CFD package. The onset of convection occurs in an isotropic homogeneous porous media, bounded by two horizontal rigid surfaces with fixed surface temperature (FST) and adiabatic vertical walls. Time-dependent simulations were conducted for bottom surface heating.

Transient Rayleigh number for unsteady-state heat conduction was defined by adopting Tan and Thorpe's (1996) transient Rayleigh number.

The onset of convection in a porous media was successfully simulated. The critical transient Rayleigh number from the simulation were in good agreement with the theoretical Rayleigh number of Lapwood (1948)  $Ra_c = 39.5$ . The maximum Nusselt numbers were in the range between 2.5 and 3.0, depending on the rate of heat transfer.

Keywords: onset of convection, transient Rayleigh number

### NOMENCLATURE

|               |  |
|---------------|--|
| $\tilde{a}_c$ | Dimensionless wave number  |
| $a$           | Wave number [ $m^{-1}$ ]   |
| $b$           | Gap between two walls of a Hele-Shaw cell [m]  |
| $d$           | Diameter of beads [m]  |
| $H$           | Total depth of fluid layer [m]   |
| $g$           | Acceleration due to gravity [ $m^2/s$ ]  |
| $h$           | Heat transfer coefficient [ $W/m^2 \text{ } ^\circ C$ ]  |
| $h_s$         | Heat transfer coefficient at surface [ $W/m^2 \text{ } ^\circ C$ ]                                       |
| $K_e$         | Permeability [ $m^2$ ]   |
| $k$           | Thermal conductivity of fluid [ $W/m \text{ } ^\circ C$ ]  |
| $k_m$         | Thermal conductivity of porous media mixture, $k_m = \phi k_f + (1-\phi)k_s$ [ $W/m \text{ } ^\circ C$ ] |
| $t_c$         | Critical time for onset of convection [s]  |
| $T$           | Temperature [ $^\circ C$ ]   |
| $T_s$         | Surface temperature at time $t$ [ $^\circ C$ ]   |
| $\Delta T$    | Temperature difference between top and bottom surface [ $^\circ C$ ]                                     |
| $\Delta T_s$  | Temperature difference of the surface of the porous media [ $^\circ C$ ]                                 |
| $Nu$          | Nusselt number   |
| $Ra$          | Rayleigh number  |
| $z$           | Penetration depth [m]  |

### Greek Symbols

|            |   |              |
|------------|---|--------------|
| $\alpha$   | Volumetric coefficient of thermal Expansion   | [ $K^{-1}$ ] |
| $\kappa$   | Thermal diffusivity   | [ $m^2/s$ ]  |
| $\kappa^*$ | Modified thermal diffusivity, $\kappa^* = k_m/(\rho C_p)_f$                                       | [ $m^2/s$ ]  |
| $\kappa_m$ | Thermal diffusivity of porous mixture, $\kappa_m = k_m/\{\phi(\rho C_p) + (1-\phi)(\rho C_p)_s\}$ | [ $m^2/s$ ]  |
| $\lambda$  | Wavelength  | [m]          |
| $\nu$      | Kinematic viscosity   | [ $m^2/s$ ]  |
| $\mu$      | Viscosity   | [Pa.s]       |
| $\rho$     | Density   | [ $kg/m^3$ ] |
| $\phi$     | Porosity  |              |

### Abbreviation

|     |  |
|-----|--|
| CFD | Computational Fluid Dynamic                  |
| FST | fixed surface temperature boundary condition |

### Subscripts

|       |                      |
|-------|----------------------|
| $c$   | critical             |
| $o$   | initial condition    |
| $max$ | maximum              |
| $f$   | fluid                |
| $s$   | solid                |
| $m$   | porous media mixture |

### INTRODUCTION

Lord Rayleigh (1916) provided the famous thermal instability criterion for the onset of buoyancy convection based on an adverse linear temperature gradient in a fluid layer. For natural convection induced by a time-dependent and non-linear temperature profile, Tan and Thorpe (1996) developed a new transient Rayleigh number for the deep fluid for various boundary conditions.

The knowledge of natural convection in a saturated porous media is of considerable interest because of its importance in modeling of the heat transfer of geothermal reservoir and engineering applications, which include the high performance insulation for building and cold storage, solar power collection.

In this study, a transient Rayleigh number based on Tan and Thorpe's (1996) theory was proposed for a semi-infinite saturated porous media with FST boundary condition. A computation fluid dynamic (CFD) package FLUENT was used to simulate the onset of convection in the porous media.

## LITERATURE REVIEW

### Linear Stability Analysis for Convection Induced in a Porous Medium

Horton and Roger (1945) and Lapwood (1948) were the early researchers who provided linear stability analyses to examine the stability breakdown of a layer of fluid subject to an adverse vertical temperature gradient in a porous medium. Lapwood (1948) suggested the inclusion of Darcy's law. Both of them had applied the Boussinesq approximation to simplify their stability analysis. Elder (1967) rearranged the thermal instability criterion of Horton and Roger (1945) and Lapwood (1948) in Rayleigh number form as shown in Table (1) for porous media and Hele-Shaw cell:

|                | Rayleigh Number   | Wave number<br>$\tilde{a}_c$ | Convective cell<br>With shape<br>of roll |
|----------------|---|------------------------------|--|
| Porous media   | $Ra = \frac{K_e g \alpha \Delta T H}{\kappa^* \nu}$     | $\pi$                        | $\frac{2\pi H}{\tilde{a}_c}$             |
| Hele-Shaw cell | $Ra = \frac{(1/12b) g \alpha \Delta T H}{\kappa_f \nu}$ | $\pi$                        | $\frac{2\pi H}{\tilde{a}_c}$             |

**Table 1:** Rayleigh number for porous media and Hele-Shaw cell for FST boundary condition

The critical Rayleigh number for various boundary conditions are summarized in Table (2).

| Boundary conditions    |                        | Author                    | Wave number | Critical Rayleigh number |
|------------------------|------------------------|---------------------------|-------------|--------------------------|
| Top surface            | Bottom surface         |                           |             |                          |
| FST, solid impermeable | FST, solid impermeable | Lapwood (1948)            | $\pi$       | 39.5                     |
| FST, free permeable    | FST, solid impermeable | Lapwood (1948)            | 2.30        | 27.1                     |
| FST, solid impermeable | CHF, solid impermeable | Ribando & Torrance (1976) | 2.30        | 27.1                     |
| FST, free permeable    | CHF, solid impermeable | Ribando & Torrance (1976) | 1.75        | 27.1                     |

**Table 2:** Summary of linear stability analysis of porous media for various boundary conditions.

### Steady-state Convection Experiments

Unfortunately all of the research reported large temperature difference between top and bottom surface in their steady-state experiments, this is in contradiction to the small disturbance required by the theory.

Morrison et al. (1949) had conducted experiments to verify the theoretical result for the bottom heating of porous media for the FST boundary condition. In their experiments they used different grade of sand saturated with water. They seemed to be unaware that the non-linear temperature profile could not be analyzed by the Rayleigh number.

Katto and Masuoka (1967) used a porous layer of 100 mm in diameter and a standard height of 9 mm in their experiments. The temperature difference across the porous layer was kept constant at about 40 - 80 °C. They found that the occurrence of convection can be predicted very well with the critical Rayleigh number provided that the thermal diffusivity was defined as  $\kappa^* = k_m / (C_p \rho)_f$ , whereas the critical Rayleigh number obtained by defining the thermal diffusivity as  $\kappa_m = k_m / \{\phi(C_p \rho)_m + (1-\phi)(C_p \rho)_f\}$  deviated from the theory. However it was in great doubt that whether their results under this extreme condition were still valid.

Elder (1967) had performed the heat transfer study in both the porous media and Hele-Shaw cell for bottom heating of FST boundary condition. In the porous media, glass spheres of diameter 3, 5, 8, 18 mm and plastic balls (styropor) 6 mm were used. However the critical temperature difference  $\Delta T_c$  and the thickness of the porous layer and the type of fluid were not reported in his paper for more detailed analysis. He claimed that the occurrence of convection was in agreement with the theoretical value  $Ra_c = 4\pi^2$ .

Later researches such as Kaneko et al. (1974) and Chen and Chen (1989) were influenced by the studies of Elder (1967) and Kato and Masuoka (1967): they applied the modified thermal diffusivity in calculating the Rayleigh number. Kaneko et al. (1974) used two different grades of silica sand with different permeability as porous media with heptane and ethanol as the saturated fluid. They found that for the system of heptane/sand B the onset of convection occurred at Rayleigh number approximately  $Ra_c = 4\pi$ . However, for the ethanol/sand systems the critical  $Ra_c$  was only 28.

Chen and Chen (1989) conducted experiments using 3mm diameter glass beads contained in a box of 24 cm x 12 cm x 4 cm. The occurrence of convection was marked by a change in the slope of the heat flux curve. They found that with a critical  $\Delta T_c = 15.2$  °C, the critical Rayleigh number was 40.07.

### Transient Convection Experiments

Elder (1968) was the pioneer who provided some analytical solutions and conducted experiments on the onset of convection in porous media. He observed an array of blobs (or plumes) rapidly growing above the lower surface (proto-sublayer), then followed by the gradual appearance of a large-scale cellular pattern of ever changing eddies. He described the development of the convection current into three distinguishable stages. i) gestation - a period of thickening of thermal layer by conduction, ii) growth - a period of rapid amplification of disturbance iii) flight- a period where the layer is dominated by buoyancy force and the eddies are accelerated out of the layer.

## THEORY OF TRANSIENT HEAT CONDUCTION IN POROUS MEDIA

The same mathematical principle advanced by Tan and Thorp (1992 and 1996) for characterizing the onset of convection induced by transient heat conduction for semi-infinite fluid are adopted here for porous media.

The transient Rayleigh number for a porous media is a function of penetration depth  $z$  and the local temperature gradient  $\partial T/\partial z$ , thus a time-dependent Rayleigh number is defined as:

$$Ra = \frac{K_e g \alpha z^2}{\kappa_m v} \left( \frac{\partial T}{\partial z} \right) \quad (1)$$

### Fixed Surface Temperature Boundary Condition (FST)

When the surface of a porous medium saturated with fluid is heated (or cooled) by a step change instantaneously to a fixed surface temperature  $T_s$ , the temperature profile in the bulk fluid of temperature  $T_o$  initially is predicted by Carslaw and Jaeger (1973) as:

$$\frac{(T - T_s)}{(T_o - T_s)} = \operatorname{erf} \left( \frac{z}{2\sqrt{\kappa_m t}} \right) \quad (2)$$

The temperature gradient can be found by differentiating equation [2]

$$\left( \frac{\partial T}{\partial z} \right)_t = - \frac{(T_o - T_s)}{\sqrt{\pi \kappa_m t}} e^{-\frac{z^2}{4\kappa_m t}} \quad (3)$$

The transient Rayleigh number as defined in Equation (1) becomes

$$Ra = \frac{K_e g \alpha z^2}{\kappa_m v} \frac{(T_o - T_s)}{\sqrt{\pi \kappa_m t}} e^{-\frac{z^2}{4\kappa_m t}} \quad (4)$$

The maximum transient Rayleigh number at any instant can be found by differentiation of equation [4] as follows.

$$\left( \frac{\partial Ra}{\partial z} \right)_t = \frac{K_e g \alpha (T_o - T_s)}{\kappa_m v \sqrt{\pi \kappa_m t}} e^{-\frac{z^2}{4\kappa_m t}} \left[ 2z - \frac{z}{2\kappa_m t} \right] = 0 \quad (5)$$

which gives the position of the maximum value of transient Ra as

$$z_{\max} = 2\sqrt{\kappa_m t} \quad (6)$$

The maximum Rayleigh number at the onset of convection may be expressed in terms of critical time  $t_c$  as:

$$Ra_{\max} = \frac{0.83 K_e g \alpha (T_o - T_s)}{v} \sqrt{\frac{t_c}{\kappa_m}} \quad (7)$$

or in the conventional form with  $\Delta T_s = (T_o - T_s)$ .

$$Ra_{\max} = \frac{K_e g \alpha \Delta T_s (0.83 \sqrt{\kappa_m t_c})}{\kappa_m v} \quad (8)$$

If  $Ra_{\max} = 4\pi^2$ , the critical time at the onset of convection can be estimated as follow:

$$t_c = 2262 \left( \frac{v \sqrt{\kappa_m}}{K_e g \alpha \Delta T_s} \right)^2 \quad (9)$$

The wavelength for a convective cell with a shape of roll and  $\tilde{a}_c$  can be predicted as:

$$\lambda = \frac{2\pi z_{\max}}{\tilde{a}_c} = 4\sqrt{\kappa_m t_c} \quad (10)$$

Whereas for a wavelength for a convective cell with a shape of circle can be predicted from:

$$\lambda = \frac{7.66 z_{\max}}{\tilde{a}_c} = 4.88 \sqrt{\kappa_m t_c} \quad (11)$$

### PROBLEM SET-UP

In this study, 2-D time-dependent simulations were carried out for a homogeneous isotropic porous layer saturated by water with FST boundary condition. The layer was bounded above and below by two rigid impermeable conducting boundaries with bottom heating. The vertical walls were adiabatic.

The top and the bottom rigid surfaces were held at an initial temperature,  $T_o = 20$  °C. At time  $t = 0$  sec, the bottom surface was suddenly heated by an increase in temperature to  $T_o + \Delta T$ , whereas the temperature at the top surface was maintained at fixed temperature  $T_o$ .

FLUENT defined the porous media model with the input of permeability, porosity and the thermal properties of the solid and the liquid. It computes the effective thermal and physical properties. The physical properties of the porous medium applied in this simulation were based on the glass beads. The porosity, density, thermal conductivity and specific heat capacity of the glass beads were assumed to be a constant as tabulated in Table (3).

| Properties                       | Glass beads |
|----------------------------------|-------------|
| Porosity                         | 0.345       |
| Density, kg/m <sup>3</sup>       | 2225        |
| Thermal conductivity, W/(m.K)    | 0.956       |
| Specific heat capacity, J/(kg.K) | 835         |

**Table 3:** Properties of porous media consisted of glass beads.

The permeability of various sizes of glass beads which were obtained by using the Kozeny-Carmen relation (Combarous and Bories 1975):

$$K_e = \frac{d^2}{172.8} \frac{\phi^3}{(1-\phi)^2} \quad (12)$$

in which  $d$  was the diameter of the glass beads and  $\phi$  the porosity.

## RESULTS AND DISCUSSION

### The Formation and Development of the Thermal Plume

The development of a thermal boundary layer until the onset of convection in the FST boundary condition can be characterized by three distinct regimes, that are quite similar to Elder's (1968) observations.

- A quasistable regime occurs in which a thermal boundary layer starts to form and thicken but no fluid motion is observed. The mechanism of heat transfer is conduction, Fig (1).
- A regime of very slow flow in which the velocity of the fluid starts to accelerate in the localized unstable points. The thermal boundary layer become distorted and marks the onset of convection, Fig (2).
- A post-onset unstable regime in which the distorted thermal boundary layer extends and forms an array of growing plumes, Fig (3). Occasionally this growing plume amalgamates with neighboring plume, extended, detached and beginning the next cycle again.

As compared to the thermal plumes of the continuous fluid, the shape of the plumes for the porous media are finger shaped without a hemispherical cap as observed at the tail side of the plumes for continuous fluid. In addition, the critical time for onset of convection and the rate of heating for the porous media are longer and larger than the continuous fluid. These differences may be due to the resistance of the beads, as the fluid has to flow and squeeze through the spaces between beads, and also the high thermal diffusivity of the glass beads.

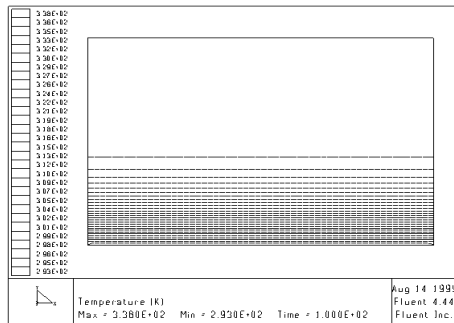


**Figure 1:** Temperature contour for 3 mm glass beads saturated with water. FST bottom heating at  $\Delta T_s = 45^\circ\text{C}$  at  $t = 100$  s

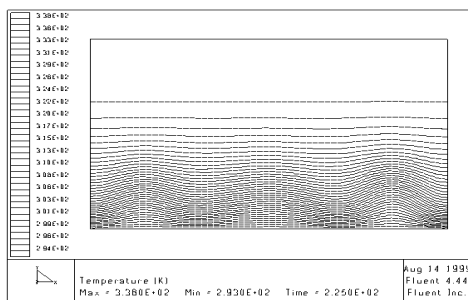


**Figure 2:** Temperature contour for 3 mm glass beads saturated with water. FST bottom heating at  $\Delta T_s = 45^\circ\text{C}$  at  $t_c = 225$  s

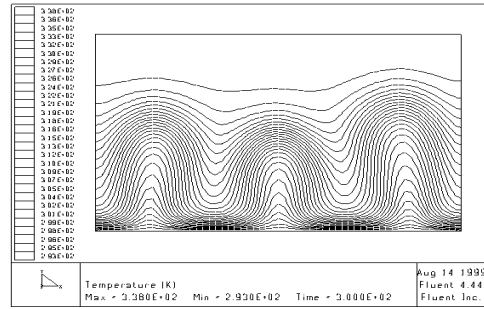


**Figure 3:** Temperature contour for 3 mm glass beads saturated with water. FST bottom heating at  $\Delta T_s = 45^\circ\text{C}$  at  $t = 300$  s

### The Critical Time and Transient Rayleigh Number

The onset of convection in the simulation is judged by observing the temperature contour, velocity magnitude, heat flux and the horizontal temperature distribution. The critical times and the transient Rayleigh numbers obtained from the simulation and theory are tabulated in Table (5).

The critical times from the simulation are in good agreement with those predicted by equation (9). The critical transient Rayleigh numbers are calculated based on the properties of the mean temperature of the bottom and the top surface and the critical times from the simulations. The average  $Ra_c$  obtained by applying  $\kappa^*$  is 38.68 and is close to the theoretical value predicted by Lapwood (1948). The average  $Ra_c$  obtained by applying  $\kappa_m$  is 30.90, which is about 22 % lower than the theoretical value.

| Beads dia. mm | $\Delta T_s$ °C | Theoretical (s) $t_c^\#$ | Theoretical (s) $t_c^*$ | Simulated (s) $t_c$ | Critical Rayleigh Number $Ra_c^\#$ | Critical Rayleigh Number $Ra_c^*$ |
|---------------|-----------------|--------------------------|-------------------------|---------------------|------------------------------------|-----------------------------------|
| 3             | 45              | 378                      | 242                     | 225                 | 30.46                              | 38.09                             |
|               | 30              | 1495                     | 955                     | 900                 | 30.63                              | 38.33                             |
| 6             | 15              | 823                      | 525                     | 450                 | 29.20                              | 36.56                             |
|               | 20              | 327                      | 209                     | 180                 | 29.27                              | 36.65                             |
| 9             | 30              | 18                       | 12                      | 15                  | 35.59                              | 44.53                             |
|               | 20              | 64                       | 41                      | 40                  | 31.14                              | 38.98                             |
| 15            | 5               | 345                      | 220                     | 180                 | 28.53                              | 35.73                             |
|               | 10              | 59                       | 38                      | 40                  | 32.38                              | 40.55                             |
| Average       |                 |                          |                         |                     | <b>30.90</b>                       | <b>38.68</b>                      |

Remark : #Rayleigh number using thermal diffusivity  $\kappa_m = k_m / [\phi (\rho C_p)_f + (1-\phi)(\rho C_p)_s]$  \*Rayleigh number using thermal diffusivity  $\kappa^* = k_m / (\rho C_p)$

**Table 5:** Critical Rayleigh numbers and critical times from simulations

### Heat Transfer and Nusselt Number

Nusselt number is defined as the ratio of heat flux by convection to the heat flux by the conduction.

Its value before the critical time is equal to 1, which represents the heat transfer in the porous media by conduction alone. After the critical time, the Nusselt number increases significantly up to a maximum value. Figures (4) and (5) show the heat flux and Nusselt number changing with time. The maximum Nusselt increases as the rate of heating is increased. Table (4) shows the maximum Nusselt number for each simulation run. The Nusselt number calculated using  $\kappa_m$  is 25% more than those calculated using  $\kappa^*$ .

| Run no. | Beads size mm | $\Delta T_s$ °C | Heat Flux, $q^o$ W/m <sup>2</sup> | Domain Size cm | FST             |                 |
|---------|---------------|-----------------|-----------------------------------|----------------|-----------------|-----------------|
|         |               |                 |                                   |                | Nu <sup>#</sup> | Nu <sup>*</sup> |
| 3       | 6             | 15              | -                                 | 3x5            | 3.10            | 2.48            |
| 6       | 9             | 20              | -                                 | 3x5            | 3.45            | 2.75            |
| 7       | 9             | 30              | -                                 | 4x6            | 4.15            | 3.32            |
| 8       | 15            | 10              | -                                 | 3x4            | 3.15            | 2.50            |
| Average |               |                 |                                   |                | <b>3.46</b>     | <b>2.76</b>     |

Remark: # Nusselt number calculated using  $\kappa_m$ , \* Nusselt number using  $\kappa^*$

**Table 4:** Maximum Nusselt number from simulations for bottom heating of FST boundary condition

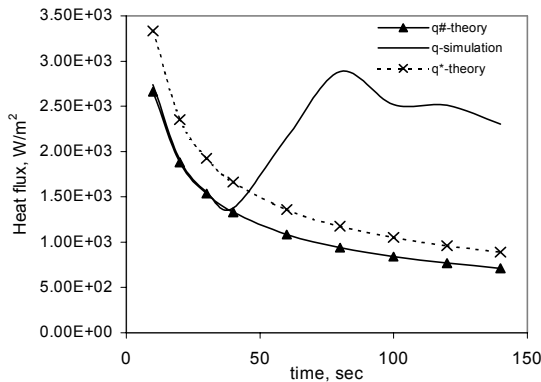


**Figure 4:** Heat flux at various times for bottom heating of FST boundary condition. (run no. 8, 15 mm glass beads,  $\Delta T_s = 10^\circ\text{C}$ , at  $t_c = 50$  sec)

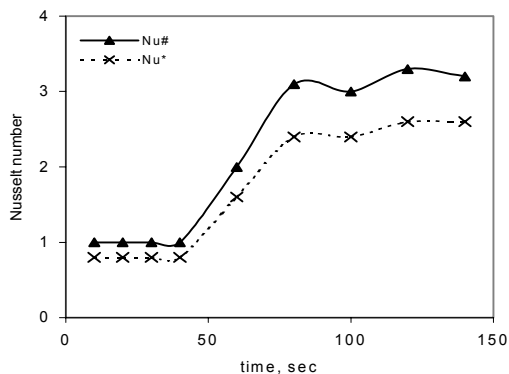


**Figure 5:** Nusselt number at various time steps (run no. 8, 15 mm glass beads,  $\Delta T_s = 10^\circ\text{C}$ , at  $t_c = 50$  sec)

## Overview

In nature, the heat transfer in porous media is more complicated than that in the continuous fluid because two media of widely different properties are conducting the heat simultaneously. Therefore, two different heat transport dynamics exist in the porous media as shown in Figure 6. Consequently, this indicates that the solid and liquid matrix in porous media are no longer in thermal equilibrium.

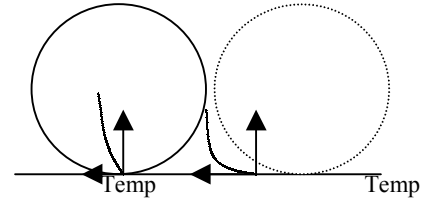


**Figure 6:** Temperature profile of the solid and liquid matrix

Beside this, the  $\Delta T_s$  required for the occurrence of convection in the porous media is considerably larger than that for the continuous fluid. This is mainly because the fluid requires more kinetic energy to overcome the large flow resistance inherent in the porous media, as the fluid has to flow around the beads. The large  $\Delta T_s$  imposed on the porous media indicated that the thermal physical properties of the porous media no longer conformed to the perturbation theory

It is clear from the foregoing consideration that the Rayleigh number can only be calculated accurately at a very strict condition where the thermal diffusivity of the solid and liquid matrix are similar and the permeability of the porous media is large enough so that  $\Delta T_s$  or heat flux will be small.

## CONCLUSION

1. The onset of convection in porous media has been successfully simulated using FLUENT.
2. A newly transient critical Rayleigh number based on Tan and Threpe's (1996) theory has been derived for onset of convection in porous media for FST boundary condition.
3. Simulations for the FST boundary condition gives the critical transient Rayleigh number based on  $\kappa^*$  close to the theoretical value of 39.5.
4. The formation and development of the thermal plume can be divided into three regimes, namely the conduction regime, the onset of convection and the post convection regime.
5. The maximum Nusselt number based on  $\kappa^*$  is in the range of 2.5 to 3.0.

## REFERENCES

- CHEN F. and CHEN C. F., (1989). "Experimental Investigation of Convective Stability in a Superposed Fluid and Porous Layers When Heated from Below". *J. Fluid Mech.* **207**, 311-321.
- ELDER J.W., (1966). "Steady Free Convection in a Porous Medium Heated from Below". *J. Fluid Mech.* **27**, 29-48.
- ELDER J.W., (1966). "Transient Convection in a Porous Medium". *J. Fluid Mech.* **27**, 609-623.
- ELDER J.W., (1967). "The Unstable Interface" *J. Fluid Mech.* **32**, 69-96.
- HORTON C.W. and ROGERS F. T. JR., (1945). "Convection Current in a Porous Media". *J. of Appl. Phys.* **16**, 367-370.
- HORTON C.W. and ROGERS F. T. JR., (1949). "Convection Current in a Porous Media II. Observation of Condition at Onset of Convection". *J. of Appl. Phys.* **20**, 1027-1029.
- KATTO. Y, MASUOKA. T., (1967). "Criterion for the Onset of Convection Flow in a Fluid in a Porous Media". *J. Heat & Mass Transfer.* **10**,297-309.
- KANEKO. T, MOHTADI M. F. and AZIZ K., (1974). "An Experiment Study of Natural Convection in Inclined Porous Media". *Int. J. Heat Mass Transfer.* **17**, 485-496.
- LAPWOOD E. R., (1948). "Convection of a Fluid in a Porous Medium". *J. Fluid Mech.*
- TAN K. K, THORPE R. B., (1999). "Onset Convection Driven by Surface Tension Caused by Transient Heat Conduction". *Chem. Eng. Science.* **54**, 775-783
- TAN K. K, THORPE R. B., (1996). "The Onset of Convection Caused by Buoyancy During Transient Heat Conduction in Deep Fluids". *Chem. Eng. Science.* **51**, 4127-4136
- TAN K. K, THORPE R. B., (1998). "The Onset of Convection Driven by Buoyancy Effects Caused by Various Modes of Transient Heat Conduction. Part 1: Transient Rayleigh Numbers". *Chem. Eng Science*, **54**, 225-238
- TAN K. K, THORPE R. B., (1998). "The Onset of Convection Driven by Buoyancy Effects Caused by Various Modes of Transient Heat Conduction. Part II: The Sizes of Plumes". *Chem. Eng. Science*, **54**, 239-244